

# BVES-AS1 suppresses the colorectal cancer progression via the miR-1269a/b-SVEP1-PI3K/AKT axis

Jianguo Yang<sup>A-F</sup>, Qican Deng<sup>B,C,F</sup>, Zhenzhou Chen<sup>B,C,F</sup>, Yajun Chen<sup>D-F</sup>, Zhongxue Fu<sup>A,D-F</sup>

Department of Gastrointestinal Surgery, The First Affiliated Hospital of Chongqing Medical University, China

A – research concept and design; B – collection and/or assembly of data; C – data analysis and interpretation;

D – writing the article; E – critical revision of the article; F – final approval of the article

Advances in Clinical and Experimental Medicine, ISSN 1899–5276 (print), ISSN 2451–2680 (online)

Adv Clin Exp Med. 2024;33(11):1217–1236

## Address for correspondence

Zhongxue Fu

E-mail: fzx19990521@126.com

## Funding sources

None declared

## Conflict of interest

None declared

Received on August 2, 2023

Reviewed on October 9, 2023

Accepted on November 9, 2023

Published online on January 17, 2024

## Abstract

**Background.** Numerous studies have indicated the engagement of long non-coding RNA (lncRNA) in various cancer types, including colorectal cancer (CRC). However, the functional and mechanistic roles of lncRNAs in CRC remain largely elusive.

**Objectives.** The aim of this study was to explore the function and mechanism of lncRNA *BVES-AS1* in CRC.

**Materials and methods.** The expression levels of *BVES-AS1* were validated in CRC tissues and paired normal samples using quantitative real-time polymerase chain reaction (qPCR). Subsequently, the biological functions of *BVES-AS1* in CRC cells were investigated both in vitro and in vivo. Various experimental techniques such as western blot, fluorescence in situ hybridization, RNA-sequencing (RNA-seq), biotin-labeled miRNA pull-down assay, dual-luciferase reporter gene assay, and RNA-protein immunoprecipitation (RIP) assay were employed to elucidate the potential mechanism of *BVES-AS1*.

**Results.** The findings of this study demonstrated that *BVES-AS1* expression was downregulated in CRC tissues compared to normal tissues, and its expression level was associated with tumor infiltration and tumor-nodule-metastasis (TNM) stage. Furthermore, *BVES-AS1* was found to suppress CRC cell proliferation, migration and metastasis both in vitro and in vivo. Mechanistically, *BVES-AS1* acted as a sponge for *miR-1269a* and *miR-1269b*, thereby regulating *SVEP1*. Additionally, the silencing of *SVEP1* activated the *PI3K/AKT* pathway.

**Conclusions.** These results suggest that *BVES-AS1* plays a crucial role in the progression of CRC through the *miR-1269a/b-SVEP1-PI3K/AKT* axis, providing new insights into the therapeutic strategies for CRC.

**Key words:** miRNA, *PI3K/AKT*, colorectal cancer, *BVES-AS1*, *SVEP1*

## Cite as

Yang J, Deng Q, Chen Z, Chen Y, Fu Z. BVES-AS1 suppresses the colorectal cancer progression via the miR-1269a/b-SVEP1-PI3K/AKT axis. Adv Clin Exp Med. 2024;33(11):1217–1236. doi:10.17219/acem/175050

## DOI

10.17219/acem/175050

## Copyright

Copyright by Author(s)

This is an article distributed under the terms of the Creative Commons Attribution 3.0 Unported (CC BY 3.0) (<https://creativecommons.org/licenses/by/3.0/>)

## Background

Colorectal cancer (CRC) is the 2<sup>nd</sup> leading cause of cancer-related deaths. The number of cancer-related deaths caused by CRC accounts for 9.4% of all cancers.<sup>1,2</sup> Local recurrence, metastasis and resistance to therapy are still the main reasons for cancer-related death in CRC.<sup>3,4</sup> At present, the mechanisms of tumorigenesis and metastasis in CRC remain unknown. Thus, clarifying the tumorigenesis, metastasis and therapeutic resistance potential molecular mechanisms of CRC is imperative.

Studies have indicated that lncRNAs can regulate CRC by serving as scaffolds, signals, decoys, or guide molecules to interact with mRNA, chromatin, miRNA, or protein.<sup>5,6</sup> It has been reported that lncRNAs participate in the proliferation, migration, invasion, and apoptosis processes of CRC. For example, *DLGAP1-AS2* mediates the ubiquitination of *Trim21* and the degradation of *ELOA* to promote CRC cell proliferation and metastasis.<sup>7</sup> lncRNAs can not only drive the progression of CRC as oncogenes but also drive the progression of CRC as tumor suppressor genes. *LINC01559* expression was downregulated in CRC. *LINC01559* overexpression inhibited CRC cell growth and invasive capacity by sponging the *miR-106b-5p* to regulate *PTEN* expression.<sup>8</sup> In addition, lncRNAs can also act as effective diagnostic biomarkers and early screening indicators of CRC.<sup>9–11</sup>

*SVEP1* is a multi-structural domain extracellular matrix protein composed of Sushi, Von Willebrand factor type A, epidermal growth factor (EGF) and pentraxin domain-containing protein 1.<sup>12</sup> Studies have suggested that *SVEP1* plays a vital function in cell adhesion, normal lymphatic vessel development and epidermal differentiation.<sup>13–16</sup> *SVEP1* and its alternative splice forms may regulate the invasive ability of breast cancer cells within the bone wall niche.<sup>17</sup> A recent study revealed that *SVEP1* levels in hepatocellular carcinoma (HCC) tissues were significantly downregulated, and high *SVEP1* expression was correlated with better progression. Mechanistically, *SVEP1* regulated the invasion and metastasis of HCC cells through the *PI3K/ATK* pathway.<sup>18,19</sup> However, the function of *SVEP1* in CRC remains unknown.

lncRNA *BVES-AS1*, located in the q21 region of chromosome 6, is the antisense strand of the protein-coding gene *BVES*. *BVES-AS1* has been found to have prognostic value in triple-negative breast cancer, with higher expression correlating with improved overall survival.<sup>20</sup> A previous study indicated that *BVES-AS1* expression was downregulated in colon cancer and can serve as a prognostic marker for colon cancer patients. However, the exact mechanism by which *BVES-AS1* affects colon cancer is still not fully understood.<sup>21</sup> In our previous analysis using The Cancer Genome Atlas (TCGA) database, we observed that the expression of *BVES-AS1* in CRC tissues was significantly lower than that in paracancerous tissues. Further bioinformatic analysis revealed a significant positive correlation between *BVES-AS1* and *SVEP1* in CRC tissues. *SVEP1* has

been shown to exhibit tumor suppression effects in various cancers. Therefore, we hypothesize that *BVES-AS1* may regulate the biological functions of CRC through its interaction with *SVEP1*.

## Objectives

The purpose of this study was to investigate the role of *BVES-AS1* in CRC and the mechanism by which *BVES-AS1* regulates *SVEP1*.

## Materials and methods

### Clinical samples

Colorectal cancer and paired paracancerous tissues were collected from patients who underwent radical surgery at the First Affiliated Hospital of Chongqing Medical University (Chongqing, China) between September 2020 and March 2021. A total of 96 CRC patients were included. The collected samples were immediately placed in liquid nitrogen for freezing and then transferred to a –80°C refrigerator for permanent storage. The clinical data of CRC patients were obtained by consulting the electronic medical record system. All included patients were confirmed to have adenocarcinoma or mucinous adenocarcinoma by pathological examination and received no neoadjuvant therapy (including chemoradiotherapy, targeted therapy or immunotherapy). In addition, patients had no other malignancies. This research protocol was reviewed and approved by the Medical Ethics Committee of the First Affiliated Hospital of Chongqing Medical University (approval No. 2020-358) and informed consent was obtained from all the study participants.

### Cell culture and transfection

Cell culture and transfection were conducted as previously reported. The human CRC cell lines SW620, HT-29, LoVo, and SW480 were acquired from the Cell Bank of the Chinese Academy of Sciences (Shanghai, China). The normal colonic epithelial cell NCM460 line was obtained from the American Type Culture Collection (ATCC; Rockville, USA). SW620, HT-29, SW480, and NCM460 cells were cultured with DMEM (Gibco, Waltham, USA), and the F12 medium (Gibco) was used to culture LoVo cells. All media were replenished with 10% fetal bovine serum (FBS; Biological Industries, Kibbutz Beit-Haemek, Israel) and 1% penicillin-streptomycin (Gibco). Small interfering RNA (siRNAs), mimics and plasmids were designed and synthesized by (RiboBio, Guangzhou, China) and transfected into SW480 and HT-29 cells using Lipofectamine 3000 (Lipo3000; Invitrogen, Waltham, USA). Lentiviruses of control and overexpression human *BVES-AS1* were

packaged by HanBio (Shanghai, China). Stable overexpression of *BVES-ASI* CRC cells after lentivirus transfection was screened with puromycin (MedChemExpress, Monmouth Junction, USA). The siRNA and mimic sequences are shown in Supplementary Table 1.

## RNA extraction and quantitative real-time PCR

The RNA extraction procedure was performed as previously described. Total RNA was extracted from CRC tissues and cells with RNAiso Plus (Takara, Shiga, Japan). A Nanodrop 2000 (Thermo Fisher Scientific, Waltham, USA) was used to analyze the extracted RNA concentration and quality. The RT Reagent Kit and SYBR Green Kit (Takara) were used for reverse transcription (RT) and quantitative real-time polymerase chain reaction (qPCR) detection, respectively. Specific stem-loop primers were designed for the reverse transcription of microRNA (Tsingke, Beijing, China). Glyceraldehyde 3-phosphate dehydrogenase (*GAPDH*) and *U6* were used as internal controls for mRNA and miRNA, respectively. The sequences of all primers are described in Supplementary Table 2. The relative RNA expression was calculated using the  $2^{-\Delta\Delta C_t}$  method.

## RNA sequencing and bioinformatics analysis

RNA-sequencing (RNA-Seq) data for CRC patients were obtained from the TCGA database (portal.gdc.cancer.gov/) in March 2021. A total of 602 cases were downloaded, of which 554 were derived from CRC and 48 cases from normal colorectal tissue. The differentially expressed lncRNAs and mRNAs were filtered using the “edgeR” packages of R software (R Foundation for Statistical Computing, Vienna, Austria) with  $|\log_2\text{foldchange}| \geq 2$  and  $p < 0.05$ . The correlation of lncRNA-mRNA or mRNA-mRNA was verified using Spearman's correlation analysis. The miRNAs targeting lncRNAs were predicted using the Lncbase (www.microrna.gr/LncBase) and miRDB (www.mirdb.org/) databases. The TargetScan (www.targetscan.org) database was used to predict the binding between mRNA and miRNA. RNA sequencing of the HT-29 vector group and *BVES-ASI* group was conducted using Illumina (Personalbio, Nanjing, China). A human genome reference was constructed based on GRCh38/hg38 of the UCSC. The R software package was used to perform the cluster and differential gene analyses. The differential mRNA was screened with  $|\log_2\text{foldchange}| \geq 1$  and  $p < 0.05$ .

## Cell Counting Kit-8 assay

The Cell Counting Kit-8 (CCK-8) assay was performed according to previously described methods.<sup>7</sup> A total of 3,000 logarithmic growth stage CRC cells were inoculated

in a 96-well plate. Ten microliters of CCK-8 solution (APEx-BIO, Houston, USA) were added at 0 h, 24 h, 48 h, and 72 h, and then incubated at 37°C for 2 h. The optical density (OD) values were measured at 450 nm using a spectrophotometer Multiskan MK3 (Thermo Fisher Scientific).

## EdU assay

The 5-ethynyl-2'-deoxyuridine (EdU) assay was performed according to the manufacturer's protocol of the EdU Cell Proliferation Kit (Beyotime Biotechnology, Shanghai, China). Colorectal cancer cells were seeded into 96-well plates and maintained for 24 h. After adding 50 mM EdU solution to the culture plates, the cells were cultured at 5% CO<sub>2</sub> and 37°C for 2 h. After fixing the cells with 4% paraformaldehyde (PFA), the cells were permeabilized with 1% Triton X-100. Azide 594 and Hoechst 33342 were used for cell staining. Photographs were taken with a fluorescence microscope (model TE2000; Nikon Corp., Tokyo, Japan).

## Wound healing assay

Colorectal cancer cells were seeded into 6-well plates and maintained until more than 90% of the cell density was reached. A sterile pipette tip formed a manual scratch on the bottom of the culture plate. Phosphate-buffered saline (PBS) was used to wash the culture plates, and the exfoliated cells were removed. Serum-free Dulbecco's modified Eagle's medium (DMEM) was used to culture cells. A microscope (model TS2; Nikon Corp.) was used to take pictures at 0 h and 24 h.

## Transwell assay

The transwell assay was conducted as previously reported.<sup>7</sup> The cells were resuspended in serum-free DMEM. The upper chamber of the transwell (Corning Company, Corning, USA) was inoculated with 200  $\mu$ L of cell suspension, while the DMEM with 15% FBS was added to lower chamber. After 48 h of incubation at 5% CO<sub>2</sub> and 37°C, 4% PFA was used to fix cells, and 1% crystal violet (Beyotime Biotechnology) was used to stain cells. In the transwell invasion assay, Matrigel (BD Biosciences, Franklin Lakes, USA) was used to cover the Transwell upper chamber before inoculating resuspended cells.

## Western blot

The protein extraction and western blot analysis were based on a previous report.<sup>7</sup> The primary antibodies including the following: rabbit *E-cadherin* antibody (#3195, Cell Signaling Technology (CST), Danvers, USA), rabbit *PI3K* antibody (#4257; CST), rabbit *N-cadherin* antibody (#13116; CST), rabbit *P-PI3K* antibody (#17366; CST), rabbit *vimentin* antibody (#5741; CST), rabbit *AKT* antibody (#2938; CST), rabbit *p-AKT* antibody (#13038; CST), and

rabbit *SVEP1* antibody (R&D Biosystems, Minneapolis, USA). Rabbit *GAPDH* antibody was purchased from Proteintech (Wuhan, China). The analysis was performed using an electrochemoluminescence (ECL) detection system (Bio-Rad, Hercules, USA).

### Apoptosis assay

The Annexin-V-FITC apoptosis detection kit (Thermo Fisher Scientific) was used for the flow cytometry apoptosis assay. The centrifuged cells were resuspended in flow cytometry binding buffer (100  $\mu$ L), and Annexin V/FITC (5  $\mu$ L) and propidium iodide (PI; 5  $\mu$ L) were used for staining. Apoptotic cells were detected using flow cytometry (CytoFLEX, Pasadena, USA).

### Fluorescence in situ hybridization

The fluorescence in situ hybridization (FISH) kit (Ribo-Bio) and *BVES-AS1* probe with Cy3 labeling (GenePharma, Shanghai, China) were used for the FISH assay. According to the protocol, Cy3-labeled *BVES-AS1* probes were incubated with CRC cells for 16 h at 37°C. Different concentrations of saline sodium citrate buffer solution was used to wash CRC cells. The nuclei of CRC cells were stained with DAPI (4',6-diamidino-2-phenylindole). A laser confocal microscope (model LSM700; Carl Zeiss, Oberkochen, Germany) was performed to take photographs.

### Dual-luciferase gene reporter assay

*BVES-AS1* and *SVEP1* 3'-untranslated region (3'-UTR) sequences wild-type (WT) and mutant (Mut), which contain *miR-1269a* and *miR-1269b* binding sites, were constructed on the pSI-Check2 plasmid vector (Hanbio, Shanghai, China). The *miR-1269a* mimics, *miR-1269b* mimics and negative control (NC) mimics were cotransfected with WT and Mut dual-luciferase gene reporter plasmids into CRC cells using Lipo3000. Luciferase activity was detected after 48 h of transfection.

### Biotin-labeled miRNA pulldown assay

Biotin-coupled *miR-1269a* mimics, *miR-1269b* mimics and NC mimics were designed and made by Sangon Biotech (Shanghai, China). Colorectal cancer cells were lysed after the biotin-labeled *miR-1269a* mimics, *miR-1269b* mimics and NC mimics were transfected for 48 h. Simultaneously, washed streptavidin magnetic beads (Invitrogen) were blocked at 4°C for 2 h. The cell lysate was added to the washed magnetic beads and incubated in the mixed solution for 12–16 h at 4°C. After washing streptavidin magnetic beads 5 times, 500  $\mu$ L of TRIzol was added to extract the RNA that specifically interacts with miRNA. Finally, the relative expression of enriched RNA was measured with qPCR.

### RNA-binding protein immunoprecipitation assay

The RIP Kit (MilliporeSigma, St. Louis, USA) was applied for RIP assays. Briefly, RIP lysis solution was used to collect and lyse CRC cells. Anti-AGO2 antibody (Proteintech) and normal rabbit IgG (MilliporeSigma) were added into the lysate, and the mixture was incubated at 4°C for 12–16 h with rotation. Subsequently, 30  $\mu$ L of Protein A/G Magnetic Bead was added and incubated with rotation for 6 h at 4°C. After washing, the enriched RNA was extracted using the TRIzol reagent.

### Xenografts in mice

The procedure of xenografts in mice was described in a previous study.<sup>7</sup> Briefly, 4–6-week-old female BALB/c nude mice were provided by Ensiweier Biotechnology Ltd. (Chongqing, China) and housed in an environment free of specific pathogenic bacteria. Ten mice were randomly assigned into 2 groups; 200  $\mu$ L ( $5 \times 10^6$ ) of HT-29 cells stably overexpressing *BVES-AS1* or empty vector was injected subcutaneously into the right axilla of nude mice. The long axes and short axes of subcutaneous tumors were measured on days 5, 10, 15, 20, and 25 after injection, and the formula:  $V = (\text{width}^2 + \text{long})/2$  was used to calculate the subcutaneous tumor volume. The mice were sacrificed on the 25<sup>th</sup> day after tumor injection. The subcutaneous tumors were extracted from the nude mice and weighed, and the mass and volume of the tumors were measured. Tumors were fixed in a 4% formalin solution for hematoxylin & eosin (H&E) staining and immunohistochemistry (IHC). All animal experiments were conducted according to the protocol approved by the Animal Experimental Research Ethics Committee of Chongqing Medicine University (approval No. IACUC-CQMU-2022-0019).

### Immunohistochemistry

The standard methods of IHC have been described in a previous study by Lu et al.<sup>22</sup> Briefly, the collected samples were fixed with a 4% formaldehyde solution. After embedding in paraffin, they were cut into 4- $\mu$ m sections. After dewaxing and hydration, the tissue sections were placed into 3% hydrogen peroxide to block the endogenous peroxidase activity. Anti-*SVEP1* antibody (R&D Biosystems) and anti-*Ki 67* antibody (Proteintech) solutions were added to the sections and incubated for 12–16 h at 4°C with anti-*SVEP1* antibody and anti-*Ki 67* antibody. The brown precipitates produced by 3,3'-diaminobenzidine (DAB) visualized the results. Finally, the sections were restained using hematoxylin. Immunohistochemistry images were obtained using a microscope (Olympus BX51; Olympus Corp., Tokyo, Japan).



## Statistical analyses

Statistical analysis was conducted using GraphPad Prism 8 (GraphPad Software, San Diego, USA) and IBM SPSS statistical software v. 25.0 (IBM Corp., Armonk, USA). All experiments were performed independently in triplicate, with each independent assay containing at least 3 samples. Mean  $\pm$  standard deviation ( $M \pm SD$ ) was used to describe normally distributed data. Normality of the data was assessed using the Shapiro–Wilk test (Supplementary Table 5), and the homogeneity of variance was tested using the Levene's test (Supplementary Table 7). For non-normally distributed paired samples, Wilcoxon signed rank analysis was

conducted. Student's t-test was used to compare 2 samples with normal distribution, while one-way analysis of variance (ANOVA) followed by Dunnett's post hoc test was applied to compare 3 or more samples with normal distribution and homogeneity of variance. If the data did not follow a normal distribution or heterogeneous variance, or the sample size was less than 9, the Mann–Whitney U test was performed to examine the data of 2 groups, and the Kruskal–Wallis test followed by Dunnett's post hoc test was used for the difference analysis of 3 or more groups (Supplementary Table 6). Spearman's correlation coefficient analysis was performed to evaluate the association between genes. The relationship between *BVES-AS1* and

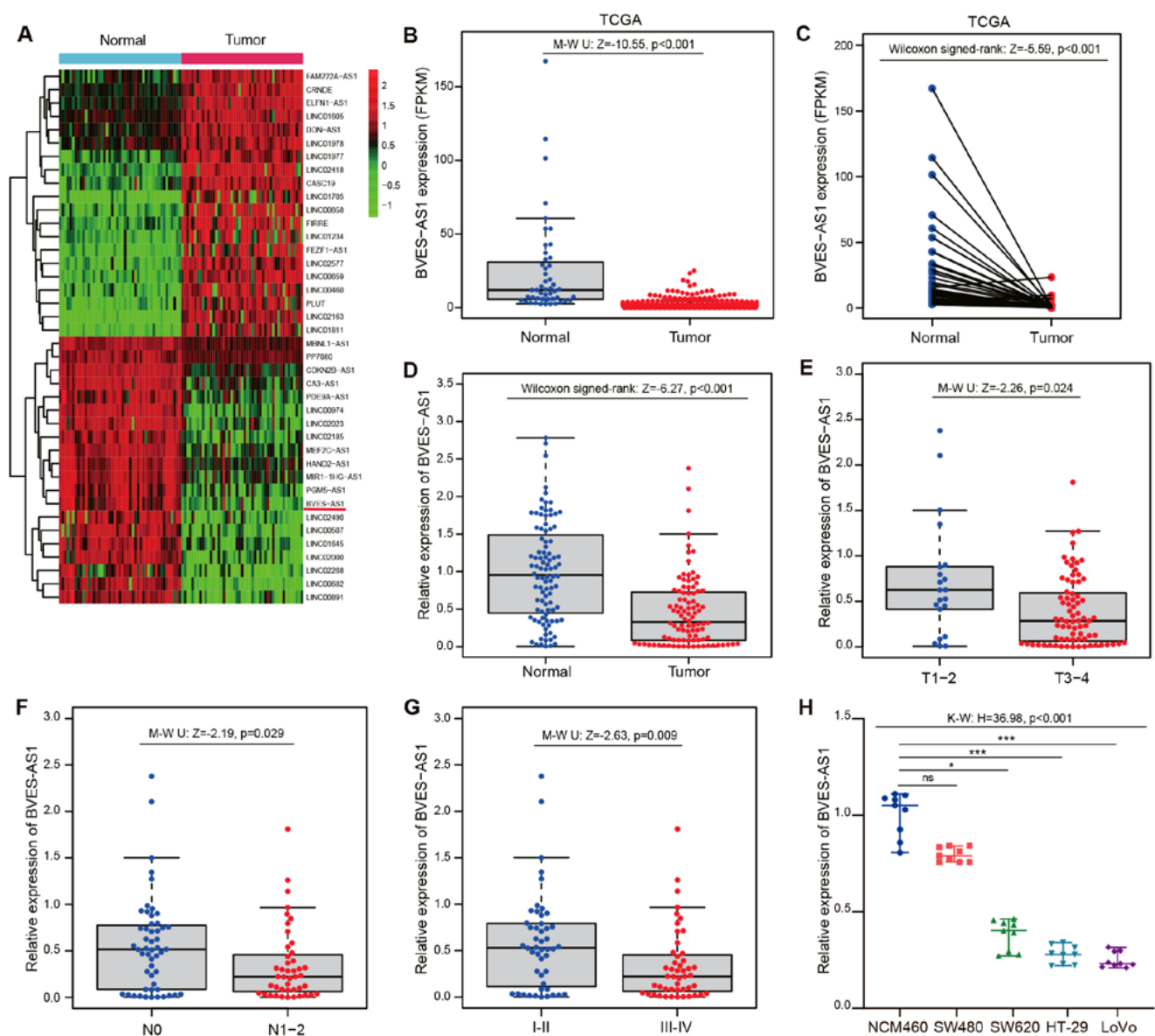


**Fig. 1.** Expression and clinical significance of *BVES-AS1* in colorectal cancer (CRC). A. Cluster heatmap showing the top 20 upregulated and top 20 downregulated lncRNAs of CRC and paired normal tissues in The Cancer Genome Atlas (TCGA) dataset ("edgeR" package of R,  $n = 47$ ); B. TCGA database was used to analyze the *BVES-AS1* expression level in 554 CRC and 48 normal tissues (Mann–Whitney U test); C. Expression of *BVES-AS1* in CRC tissues and matched normal tissues in the TCGA database (Wilcoxon signed-rank,  $n = 47$ ); D. Expression of *BVES-AS1* in CRC tissues and paired adjacent tissues (Wilcoxon signed-rank,  $n = 96$ ); E–G. Expression of *BVES-AS1* was estimated according to T stage, lymph node metastasis and pathological stage (Mann–Whitney U test,  $n = 96$ ); H. Expression of *BVES-AS1* in colonic epithelial cells and 4 CRC cell lines (Kruskal–Wallis test with Dunn's post hoc test,  $n = 9$ , \* $p < 0.05$ , \*\* $p < 0.01$ , \*\*\* $p < 0.001$ ). Data are presented as median with range. All assays were conducted in triplicate

the baseline clinical characteristics of CRC patients was analyzed using the  $\chi^2$  or Fisher's exact test. A p-value of less than 0.05 ( $p < 0.05$ ) was considered statistically significant.

## Results

### *BVES-AS1* is downregulated in CRC and related to pathological stage

The bioinformatics analysis of TCGA data revealed 720 lncRNAs that were upregulated, and 293 lncRNAs that were downregulated in CRC tissue based on  $|\log_2\text{fold change}| \geq 2$  and  $p < 0.05$ . The clustering heatmap showed the dysregulated genes in 47 paired CRC and normal colorectal tissues (Fig. 1A). The differential expression gene analysis showed that *BVES-AS1* expression in paracancerous tissue was significantly higher than that in CRC tissue (Fig. 1B,C). The 96 CRC tissues and paracancerous tissues were gleaned and analyzed. The results showed that *BVES-AS1* expression in CRC tissues was significantly downregulated compared with that in paracancerous tissues (Fig. 1D). The clinical baseline analysis of CRC patients indicated that *BVES-AS1* expression was closely associated with the tumor infiltration ( $p = 0.024$ ), lymph node positivity ( $p = 0.029$ ) and tumor-nodule-metastasis (TNM) stage ( $p = 0.009$ ) (Fig. 1E–G, Supplementary Table 3). Furthermore, *BVES-AS1* was significantly downregulated in LoVo, HT29, SW480, and SW620 cells compared with NCM460 cells (Fig. 1H).

### *BVES-AS1* inhibits CRC cell proliferation and invasion in vitro

The previous results indicated that *BVES-AS1* expression was downregulated in HT-29 cells, but relatively high in SW480 cells (Fig. 1H). Hence, SW480 and HT-29 cells were used in subsequent studies. To elucidate the effect of *BVES-AS1* on CRC biological function, HT-29 and SW480 cells with stable overexpression of *BVES-AS1* and vector were constructed by lentivirus infection (Fig. 2A). In addition, *BVES-AS1* expression in SW480 cells was knocked down by si-BVES-AS1#1, and si-BVES-AS1#2 (Fig. 2B). Cell Counting Kit-8 and EdU assays showed that *BVES-AS1* overexpression prominently suppressed HT-29 and SW480 cell proliferation while silencing *BVES-AS1* promoted SW480 cell viability (Fig. 2C–F, Supplementary Fig. 1A–C). Transwell and wound healing assay results indicated that the migration and invasion abilities of CRC cells were significantly suppressed by upregulated *BVES-AS1* (Fig. 3A,C, Supplementary Fig. 1D–G). In contrast, the migration and invasion abilities of SW480 cells were enhanced by *BVES-AS1* knockdown (Fig. 3B,D). Meanwhile, western blot analysis revealed that *BVES-AS1* upregulation significantly downregulated *N-cadherin* and *vimentin* levels while silencing *BVES-AS1* produced

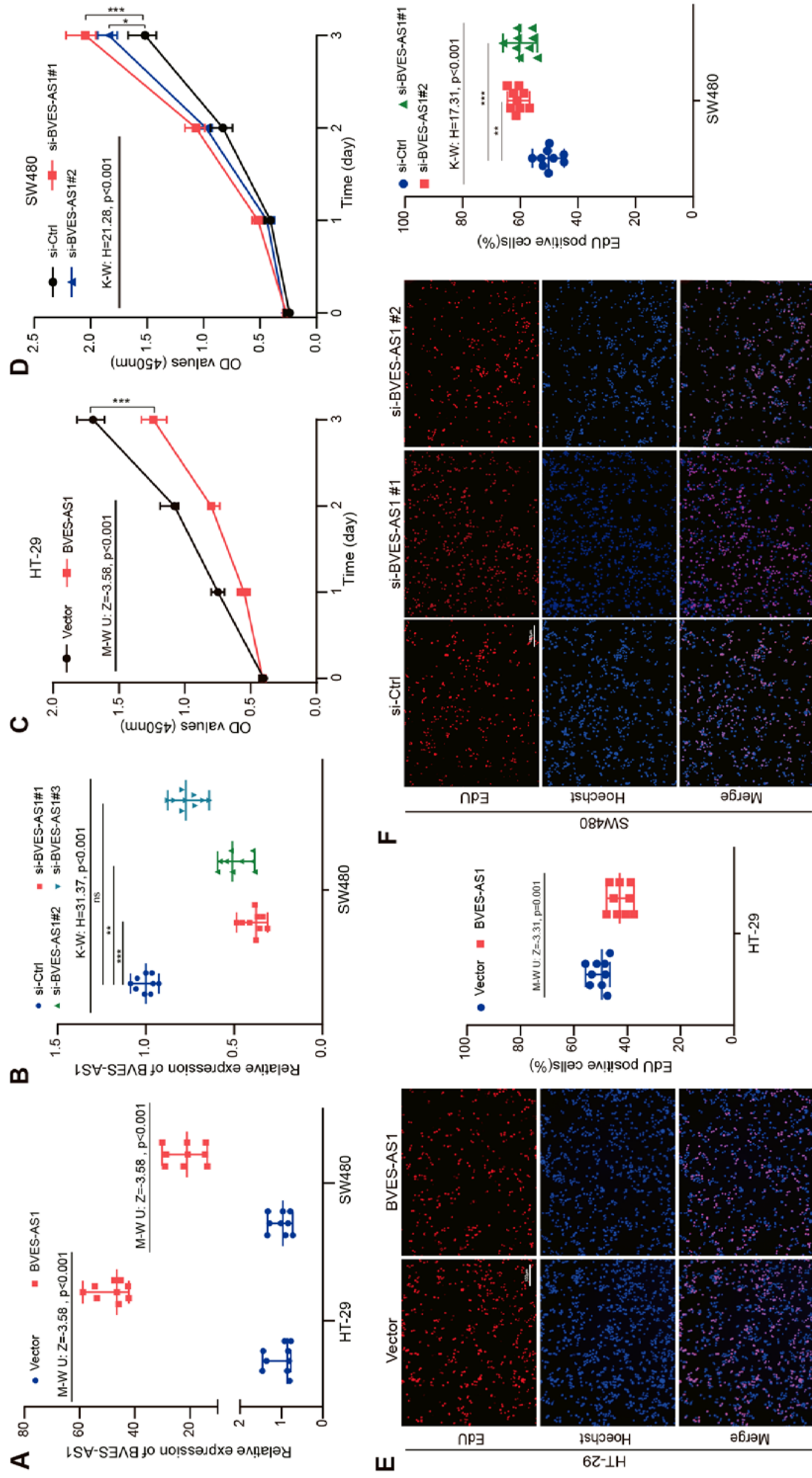
the opposite effects (Fig. 4E,F). Flow cytometry apoptosis assays indicated that the overexpression of *BVES-AS1* contributed to SW480 and HT-29 cell apoptosis (Fig. 4A,B, Supplementary Fig. 1H,I). *BVES-AS1* downregulation inhibited SW480 cell apoptosis (Fig. 4C,D). In general, *BVES-AS1* acted as a tumor suppressor gene to inhibit CRC cell biological roles in vitro.

### *BVES-AS1* functions as a sponge for *miR-1269a* and *miR-1269b*

To clarify the mechanism of *BVES-AS1*, we employed nuclear-cytoplasmic fractionation and FISH assays and observed that *BVES-AS1* was mainly distributed in the cytoplasm of HT-29 and SW480 cells (Fig. 5A,B). Next, we used the miRDB and LncBase databases to predict miRNAs that may bind to *BVES-AS1*. The predicted results revealed that *BVES-AS1* contained *miR-1269a* and *miR-1269b* binding sites (Fig. 5C). Unexpectedly, the seed sequences of *miR-1269a* and *miR-1269b* were identical (Fig. 5J). The study also found that compared with normal colorectal tissue, the *miR-1269a* and *miR-1269b* levels in CRC were upregulated (Fig. 5D,F). Correlation analysis demonstrated that *miR-1269a* and *miR-1269b* expression had a negative correlation with *BVES-AS1* expression in CRC (Fig. 5E,G). In addition, overexpression of *miR-1269a* and *miR-1269b* in HT-29 and SW480 cells significantly downregulated *BVES-AS1* mRNA levels (Fig. 5H,I). To further explain the relationship between *miR-1269a*, *miR-1269b* and *BVES-AS1*, the WT and Mut dual-luciferase reporter gene plasmids of *BVES-AS1* were constructed and synthesized. (Fig. 5J). The *miR-1269a* mimics, *miR-1269b* mimics or NC mimics were cotransfected with WT or Mut plasmids into HT-29 and SW480 cells to detect luciferase activity. The results indicated that the *miR-1269a* or *miR-1269b* mimics could significantly inhibit luciferase activity in the WT group compared with the NC mimics. In contrast, the luciferase activity in the Mut group was not significantly different (Fig. 6A–D). Biotinylated *miR-1269a* mimic and *miR-1269b* mimic WT probes, and Mut probes were designed and synthesized for a biotin-coupled microRNA capture assay. The results indicated that *BVES-AS1* in the WT probe group was significantly enriched in HT-29 cells (Fig. 6E,F). In addition, RIP experiments further found that compared with the immunoglobulin G (IgG) group, the enrichment of *BVES-AS1*, *miR-1269a* and *miR-1269b* was significantly higher (Fig. 6G). Our data suggested that *BVES-AS1* may function as a sponge for *miR-1269a* and *miR-1269b* in CRC cells.

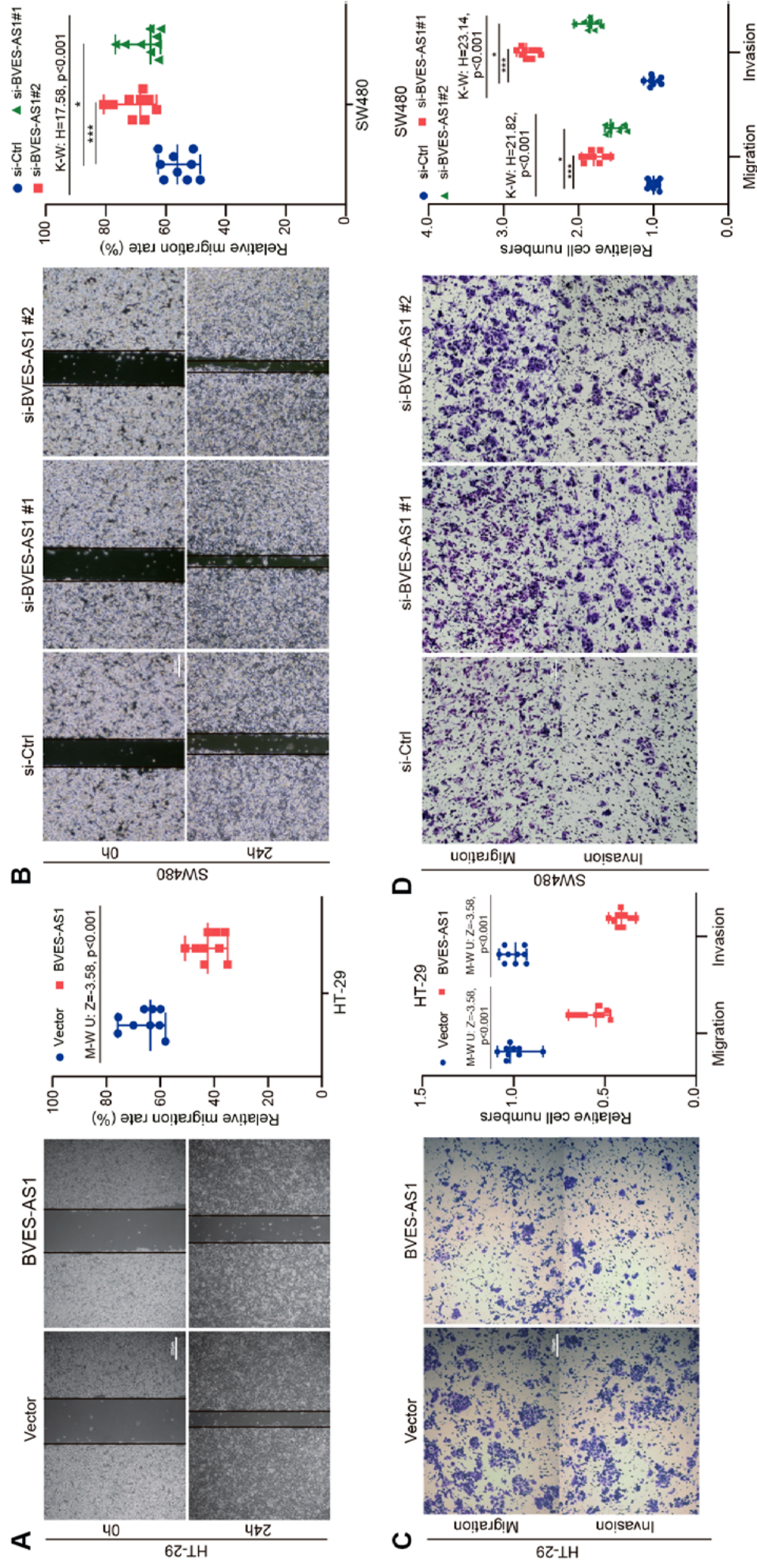
### *BVES-AS1* reverses the oncogenic effect of *miR-1269a* and *miR-1269b*

To evaluate whether *BVES-AS1* can inhibit the biological function of CRC cells by sponging *miR-1269a* or *miR-1269b*, rescue experiments were performed. The results



**Fig. 2.** *BVES-AS1* inhibits CRC cell proliferation in vitro. A,B. *BVES-AS1* overexpression and downregulation were verified with qualitative real-time polymerase chain reaction (qPCR); C,D. The proliferation curves of colorectal cancer (CRC) cells with upregulation or knockdown of *BVES-AS1* were detected using the Cell Counting Kit-8 (CCK-8) assay at 0 h, 24 h, 48 h, and 72 h; E,F. 5-Ethynyl-2'-deoxyuridine (EdU) assay was conducted to evaluate the proliferation ability of CRC cells after overexpression or silencing *BVES-AS1*; A,C,E. The results were statistically analyzed using the Mann-Whitney U test ( $n = 9$ ); B,D,F. The results were analyzed using the Kruskal-Wallis test with Dunn's post hoc test ( $n = 9$ ). \* $p < 0.05$ , \*\* $p < 0.01$ , \*\*\* $p < 0.001$ . The data are presented as median with range. All assays were conducted in triplicate.







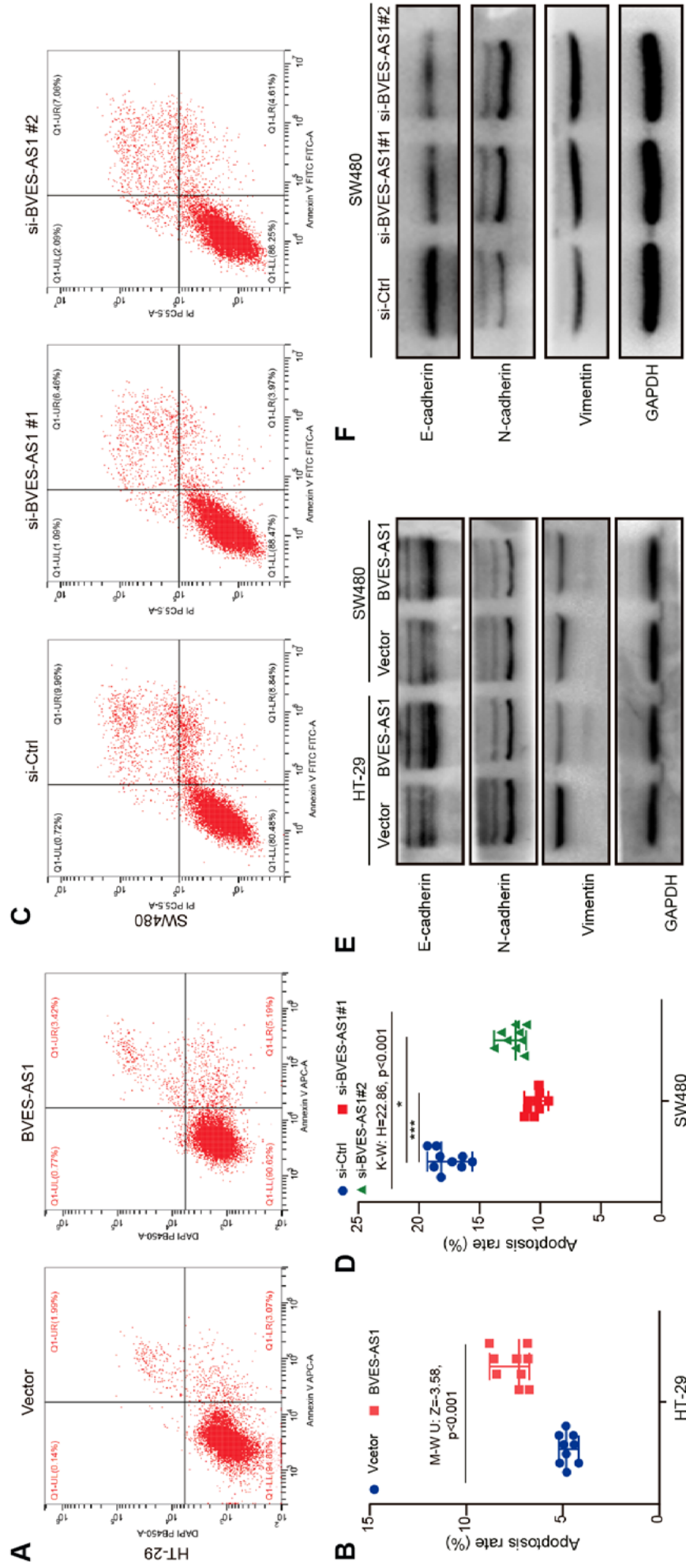


**Fig. 4.** *BVES-AS1* induces and suppresses epithelial-mesenchymal transition (EMT) of colorectal cancer (CRC) cells in vitro. A–D. Apoptosis of CRC cells silenced and overexpressed *BVES-AS1*; it was detected using flow cytometry; E, F. EMT markers (*E-cadherin*, *N-cadherin*, and *vimentin*) were detected with western blot after *BVES-AS1* overexpression or downregulation; B. The results were statistically analyzed using the Mann–Whitney U test ( $n = 9$ ); C. The results were analyzed using the Kruskal–Wallis test with Dunn's post hoc test ( $n = 9$ ). \* $p < 0.05$ , \*\* $p < 0.01$ , \*\*\* $p < 0.001$ . The data are presented as median with range. All assays were conducted in triplicate

A. Fluorescence in situ hybridization (FISH) was used to detect the localization of *BVES-AS1* in HT-29 and SW480 cells.

The nucleus was stained with 4',6-diamidino-2-phenylindole

cells was analyzed with quantitative real-time polymerase chain

were predicted using miRDB and LncBase; DE Expression

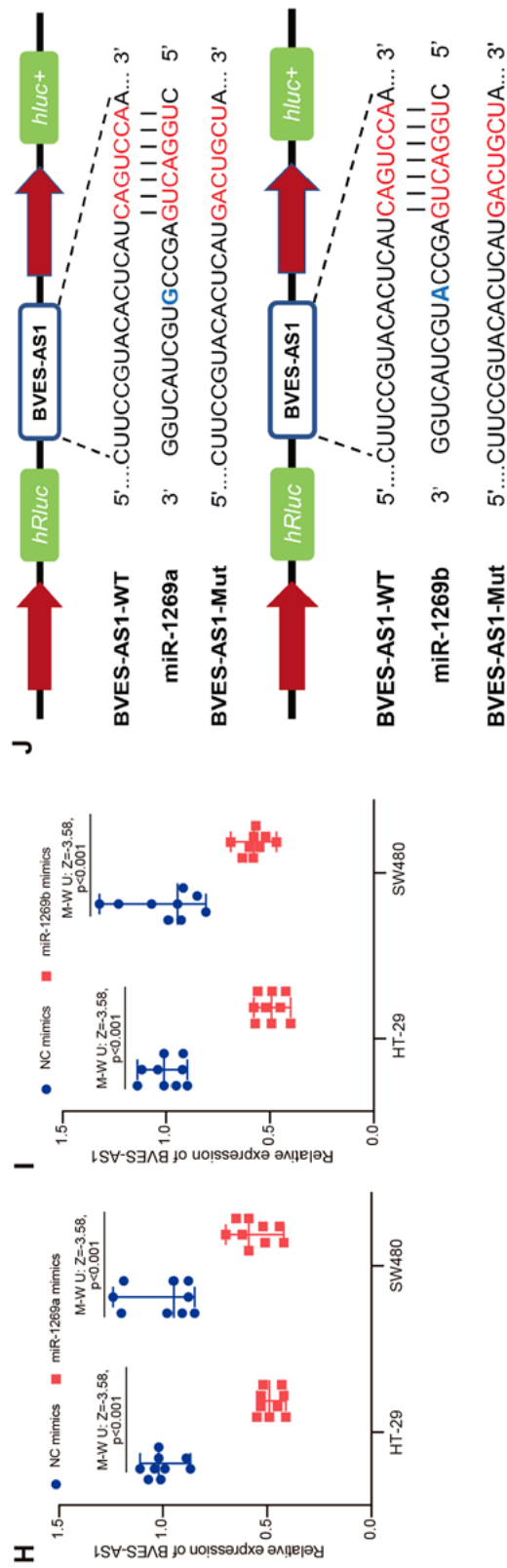
colorectal cancer (CRC) tissues and paired adjacent tissues

analysis showed that the expressions of *BVES*, *AS1* and *miR-1269a*

(Spearman's correlation coefficient,  $n = 96$ ); H<sub>1</sub>. The change of BVES

J. Schematic diagram of *BVES-AS1* wild-type (WT) and mutant (Mut)

range, and all assays were performed in triplicate



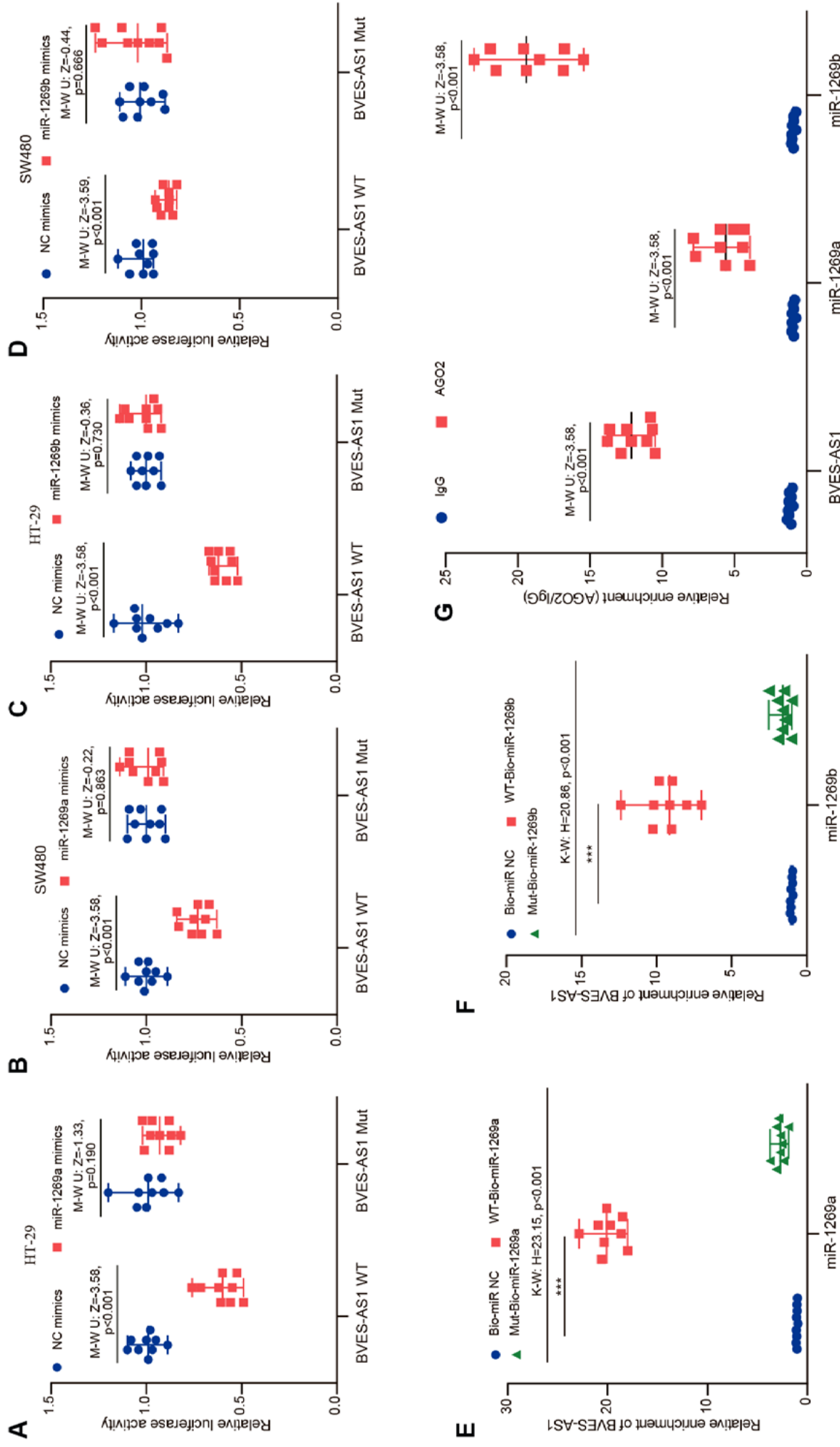


**Fig. 6.** *BVES-AS1* functions as a sponge for *miR-1269a* and *miR-1269b*. A–D. Wild-type (WT) or mutant (Mut) *BVES-AS1* luciferase reporter gene vectors were co-transfected with *miR-1269a* or *miR-1269b* mimics, and the luciferase activity was determined (Mann–Whitney U test,  $n = 9$ ). E, F. Biotin-labeled miRNA pull-down assay showed the enrichment level of *BVES-AS1* captured by biotinylated *miR-1269a/b* mimics or negative control (NC) mimics (Kruskal–Wallis test with Dunn’s post hoc test,  $n = 9$ ; \*\*\*  $p < 0.001$ ). G. RNA immunoprecipitation (RIP) assay showed the fold enrichment of *BVES-AS1*, *miR-1269a*, and *miR-1269b* in HT-29 cells (Mann–Whitney U test,  $n = 9$ ). The data are presented as median with range, and all assays were performed in triplicate.



indicated that the *miR-1269a* and *miR-1269b* mimics promoted CRC cell proliferation and vitality while transfecting the *BVES-AS1* plasmid partially eliminated the proliferation ability induced by *miR-1269a* mimics or *miR-1269b* mimics (Supplementary Fig. 2A–D). Transwell and wound healing assays indicated that compared with NC mimics, the overexpression of *miR-1269a* and *miR-1269b* advanced CRC cell migration and invasion ability. The migration and invasion mediated by *miR-1269a* and *miR-1269b* mimics were also attenuated by upregulated *BVES-AS1* (Supplementary Fig. 2E–I). Western blot analysis showed that *E-cadherin* levels were partially downregulated in CRC cells after cotransfecting with *miR-1269a* mimics, *miR-1269b* mimics and *BVES-AS1*. In contrast, *N-cadherin* and *vimentin* protein levels showed the opposite results (Supplementary Fig. 2L). Furthermore, inhibition of apoptosis induced by *miR-1269a* mimics or *miR-1269b* mimics was also reversed by upregulated *BVES-AS1* (Supplementary Fig. 2J,K). In summary, these results demonstrate that *BVES-AS1* can reverse the oncogenic effect of *miR-1269a* and *miR-1269b* in CRC cells.

### **SVEP1 is the common downstream target of *miR-1269a* and *miR-1269b***

To further elucidate how *BVES-AS1* regulated CRC cell function through *miR-1269a* and *miR-1269b*, we performed RNA-seq on HT-29 cells transfected with *BVES-AS1* overexpression plasmid and vector plasmid. The results showed that compared with the vector group, 35 upregulated genes and 59 downregulated genes were detected in the *BVES-AS1* overexpression group ( $|\log_2\text{-fold change}| \geq 1$ ,  $p < 0.05$ ) (Fig. 7A, Supplementary Table 4). The TargetScan database and RNA-seq data were applied to prognosticate the target genes of *miR-1269a* and *miR-1269b*. The predicted results indicated that *SVEP1* had binding sites for *miR-1269a* and *miR-1269b* (Fig. 7B). In the TCGA database, *SVEP1* was significantly downregulated in CRC tissue (Fig. 7C). The qPCR detection of 96 CRC samples and matched adjacent samples suggested that the mRNA level of *SVEP1* in CRC was also decreased (Fig. 7D). Correlation analysis indicated that *SVEP1* in CRC tissues was significantly positively correlated with *BVES-AS1* ( $R = 0.615$ ) (Fig. 7E). In contrast, *SVEP1* was negatively correlated with *miR-1269a* ( $R = 0.545$ ) and *miR-1269b* ( $R = 0.545$ ) in CRC (Fig. 7F,G). The qPCR and western blotting indicated that *SVEP1* was upregulated at the mRNA and protein levels by *BVES-AS1* overexpression in CRC cells (Fig. 7I,K). As expected, *miR-1269a* and *miR-1269b* mimics in CRC cells significantly downregulated the expression of *SVEP1* (Fig. 7H,J). To verify the relationship among *SVEP1*, *miR-1269a* and *miR-1269b*, we constructed *SVEP1* 3'-UTR WT and Mut dual-luciferase reporter gene plasmids (Fig. 8A,B). The luciferase assay revealed that the luciferase activity of CRC cells transfected with the *SVEP1* WT plasmid was inhibited by *miR-1269a* and

*miR-1269b* mimics. In contrast, no significant difference was detected in the *SVEP1*-Mut plasmid (Fig. 8C–F). These results indicated that *SVEP1* is the common target gene of *miR-1269a* and *miR-1269b*.

### **SVEP1 suppresses the function of CRC cells through the *PI3K/AKT* pathway**

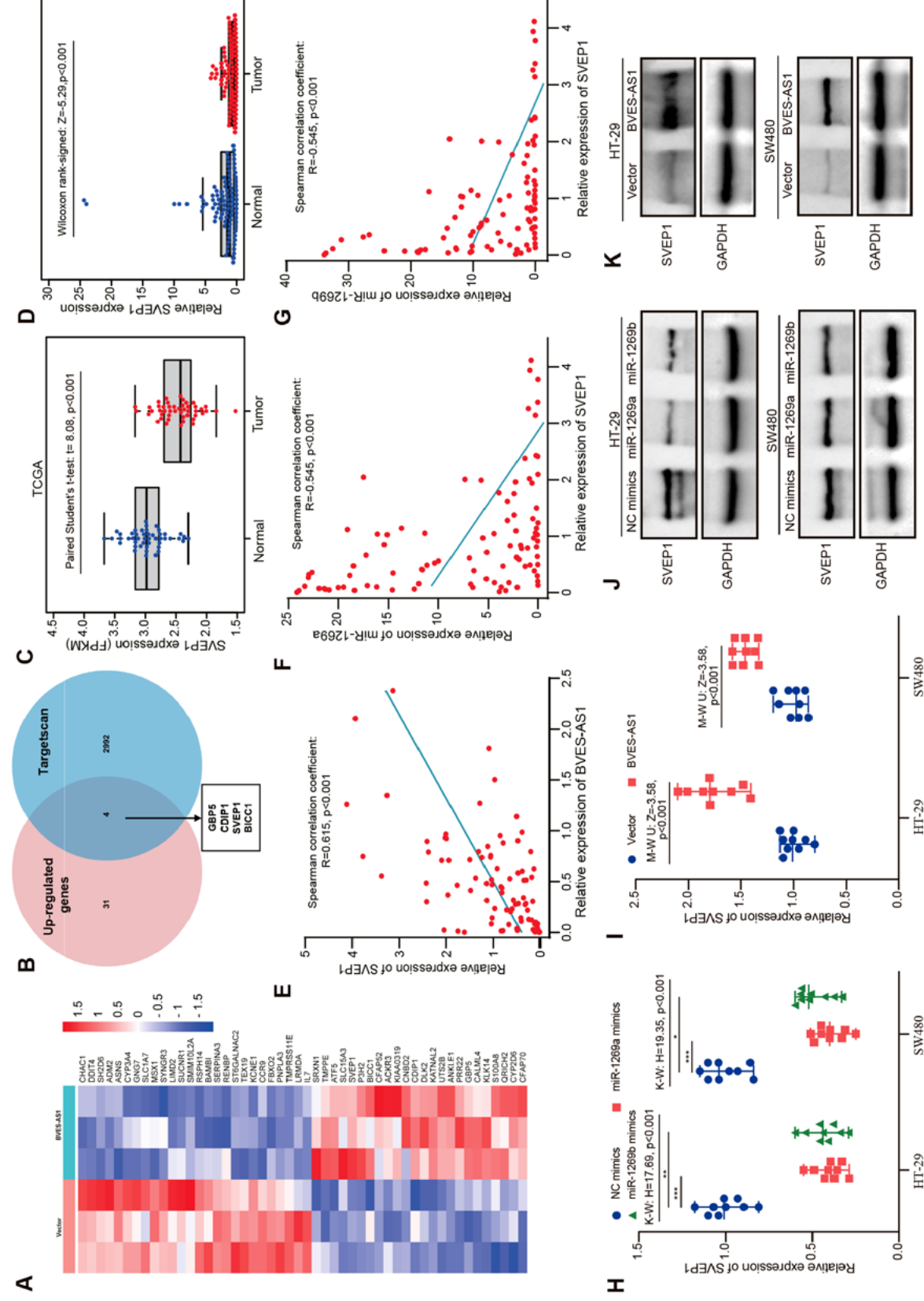
The biological role of *SVEP1* in CRC is still unknown. We performed functional experiments in CRC cells by knocking down *SVEP1* with siRNA to elucidate the role of *SVEP1* (Fig. 9A, Supplementary Fig. 3A). Subsequently, EdU and CCK-8 assays indicated that compared with si-ctrl transfection, *SVEP1* knockdown promoted HT-29 and SW480 cell proliferation (Fig. 9B–E). The si-SVEP1#1 and si-SVEP1#2 also enhanced CRC cell migration and invasion (Fig. 9F–H, Fig. 10A, Supplementary Fig. 3B). Western blot analysis indicated that *SVEP1* knockdown in CRC cells significantly promoted EMT (Fig. 10C). Moreover, downregulating *SVEP1* also inhibited the apoptosis of CRC cells (Fig. 10B, Supplementary Fig. 3C). The results demonstrated that *SVEP1* has a tumor suppressor function in CRC cells.

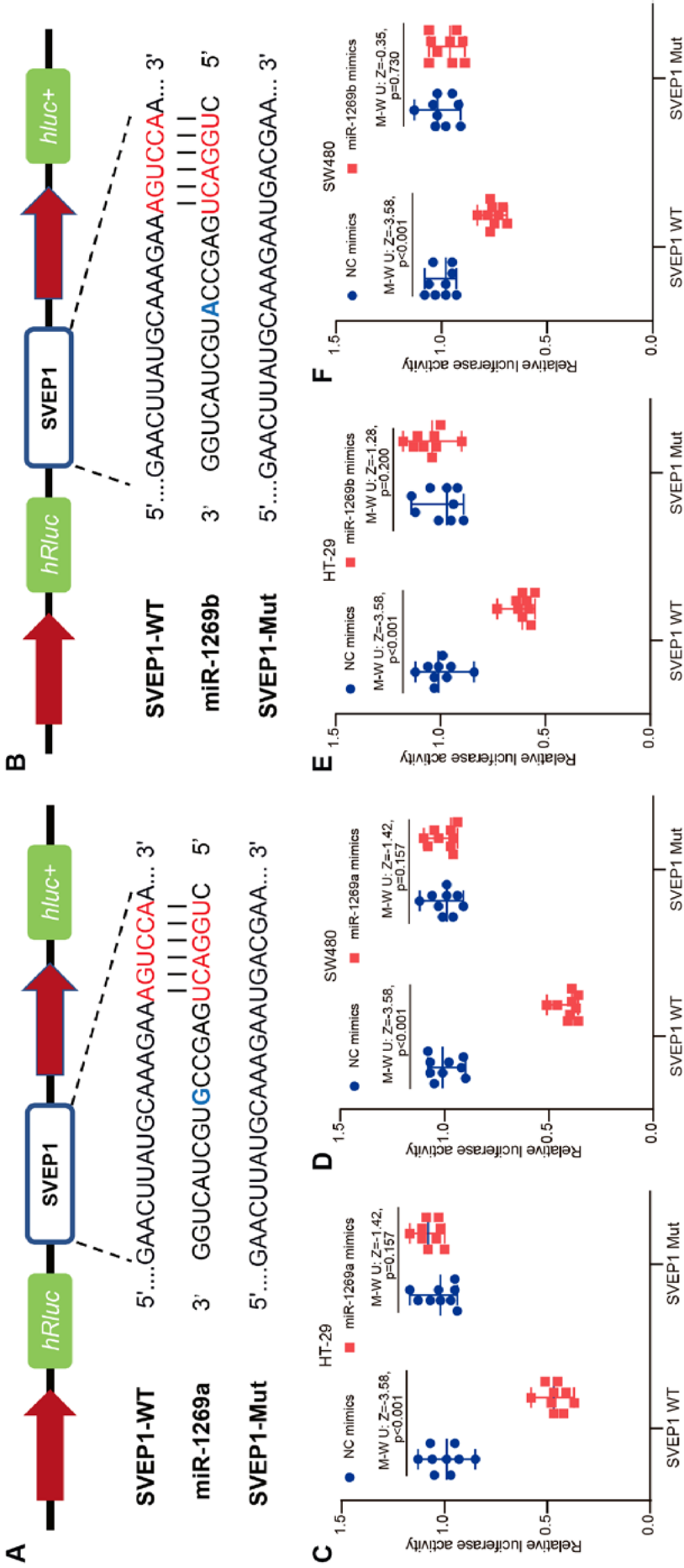
A previous study mentioned that *SVEP1* knockdown promoted proliferation, bone infiltration and lung metastasis of HCC cells by activating the *PI3K/AKT* pathway.<sup>18</sup> Therefore, we discussed whether *BVES-AS1* could regulate the *PI3K/AKT* pathway through the *miR-1269a/miR-1269b-SVEP1* axis in CRC cells. Western blotting revealed that *BVES-AS1* upregulation decreased the levels of phosphorylated *AKT* and *PI3K* in CRC cells (Fig. 10D). In CRC cells, transfection of *miR-1269a* and *miR-1269b* mimics also upregulated p-*AKT* and p-*PI3K* levels (Fig. 10E). Furthermore, *SVEP1* silencing significantly enhanced the levels of phosphorylated *AKT* and *PI3K* in CRC cells (Fig. 10F). Rescue experiments showed that *miR-1269a* or *miR-1269b* could partially restore the downregulation of phosphorylated *AKT* and *PI3K* caused by the upregulation of *BVES-AS1* (Fig. 10G). Silencing *SVEP1* also partially restored the decrease in p-*AKT* and p-*PI3K* in CRC caused by overexpression of *BVES-AS1* (Fig. 10H). The data indicated that *BVES-AS1* regulated the *PI3K/AKT* pathway through the *miR-1269a/miR-1269b-SVEP1* axis (Fig. 11G).

### **BVES-AS1 inhibits the proliferation of CRC cells in vivo**

To verify the impact of *BVES-AS1* on CRC cell proliferation in vivo, HT-29 cells stably overexpressing *BVES-AS1* or the vector were xenografted into nude mice by right axilla subcutaneous injection to form an animal model. The size of the xenograft tumor was measured 5, 10, 15, 20, and 25 days after tumor cell injection. The xenograft tumors were harvested on the 25<sup>th</sup> day (Fig. 11A). Compared with the vector group, the *BVES-AS1* group had smaller tumor volumes and slower tumor growth in xenografts (Fig. 11B–D).

**Fig. 7. The correlation of *SVEP1* with *miR-1269a* and *miR-1269b*.**  
**A.** The cluster heatmap showing the top 20 upregulated and top 20 downregulated mRNA of RNA-sequencing ("edgeR" package of R, n = 6); **B.** Four potential target mRNAs of *miR-1269a* and *miR-1269b* were predicted using RNA-sequencing and Targetscan; **C.** Expression of *SVEP1* in colorectal cancer (CRC) samples and paired normal samples in The Cancer Genome Atlas (TCGA) database (paired Student's t-test; n = 47); **D.** Expression of *SVEP1* in CRC tissues and matched adjacent tissues (Wilcoxon signed-rank test, n = 96); **E.** The correlation analysis of *BVES-AS1* level and *SVEP1* level in CRC tissues (Spearman's correlation coefficient, n = 96); **F.** The correlation analysis of *miR-1269a* or *miR-1269b* level and *SVEP1* level in CRC tissues (Spearman's correlation coefficient, n = 96); **G.** The mRNA and protein level of *SVEP1* after *BVES-AS1*, *miR-1269a*, or *miR-1269b* overexpression (Mann-Whitney U test and Kruskal-Wallis test with Dunn's post hoc test, n = 9; \*p < 0.05, \*\*\*p < 0.01, \*\*\*\*p < 0.001). The data are presented as median with range. All assays were conducted in triplicate

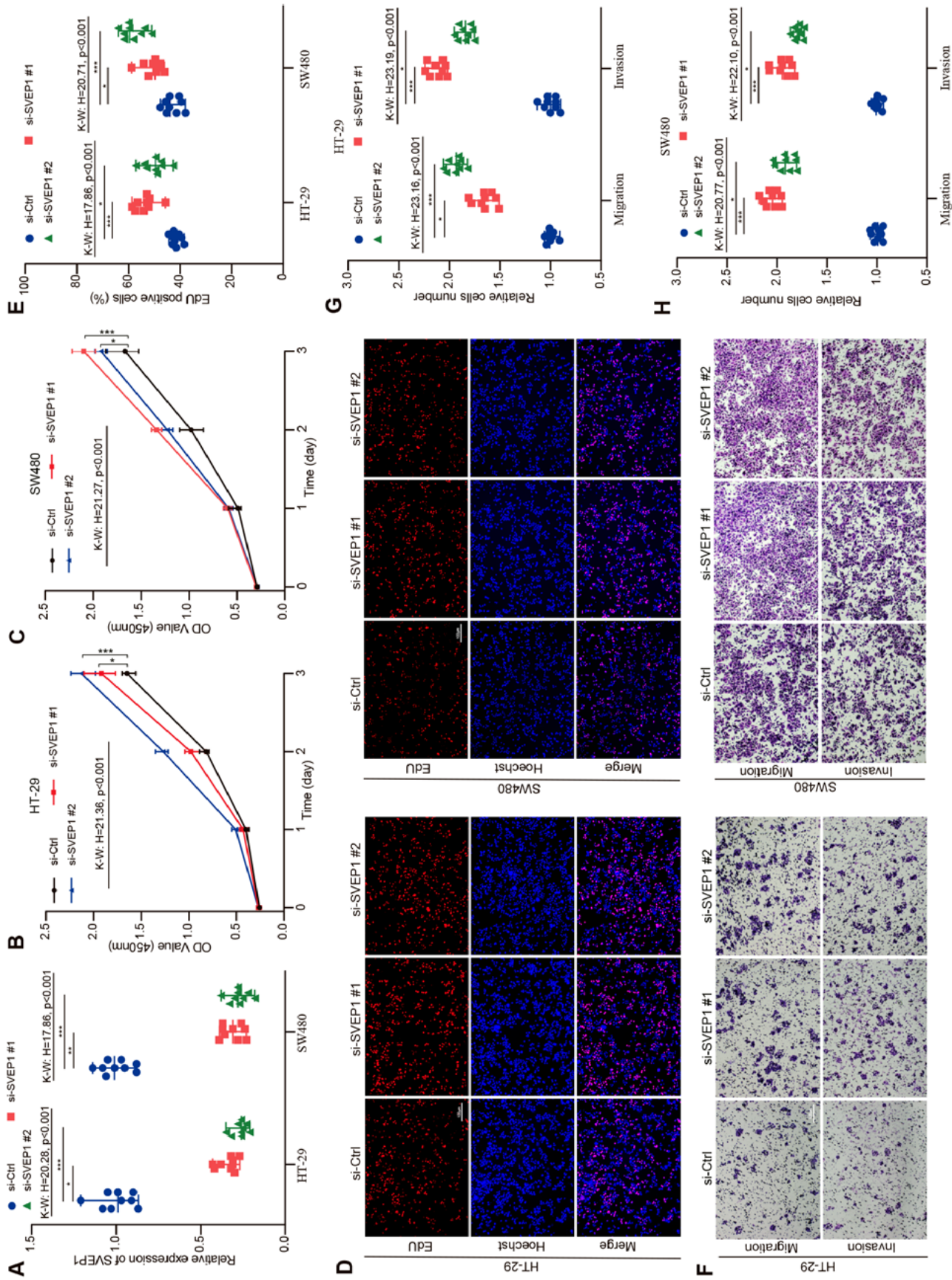




**Fig. 8.** *SVEP1* is the common downstream target of *miR-1269a* and *miR-1269b*. A,B. Schematic diagram of *SVEP1* 3'-UTR and mutant (Mut) luciferase reporter gene vectors; D-F. Luciferase assay in colorectal cancer (CRC) cells co-transfected WT or Mut *SVEP1* plasmid together with *miR-1269a* mimics or *miR-1269b* mimic or negative control (NC) mimics (Mann-Whitney U test, n = 9). The data are presented as median with range. All assays were conducted in triplicate

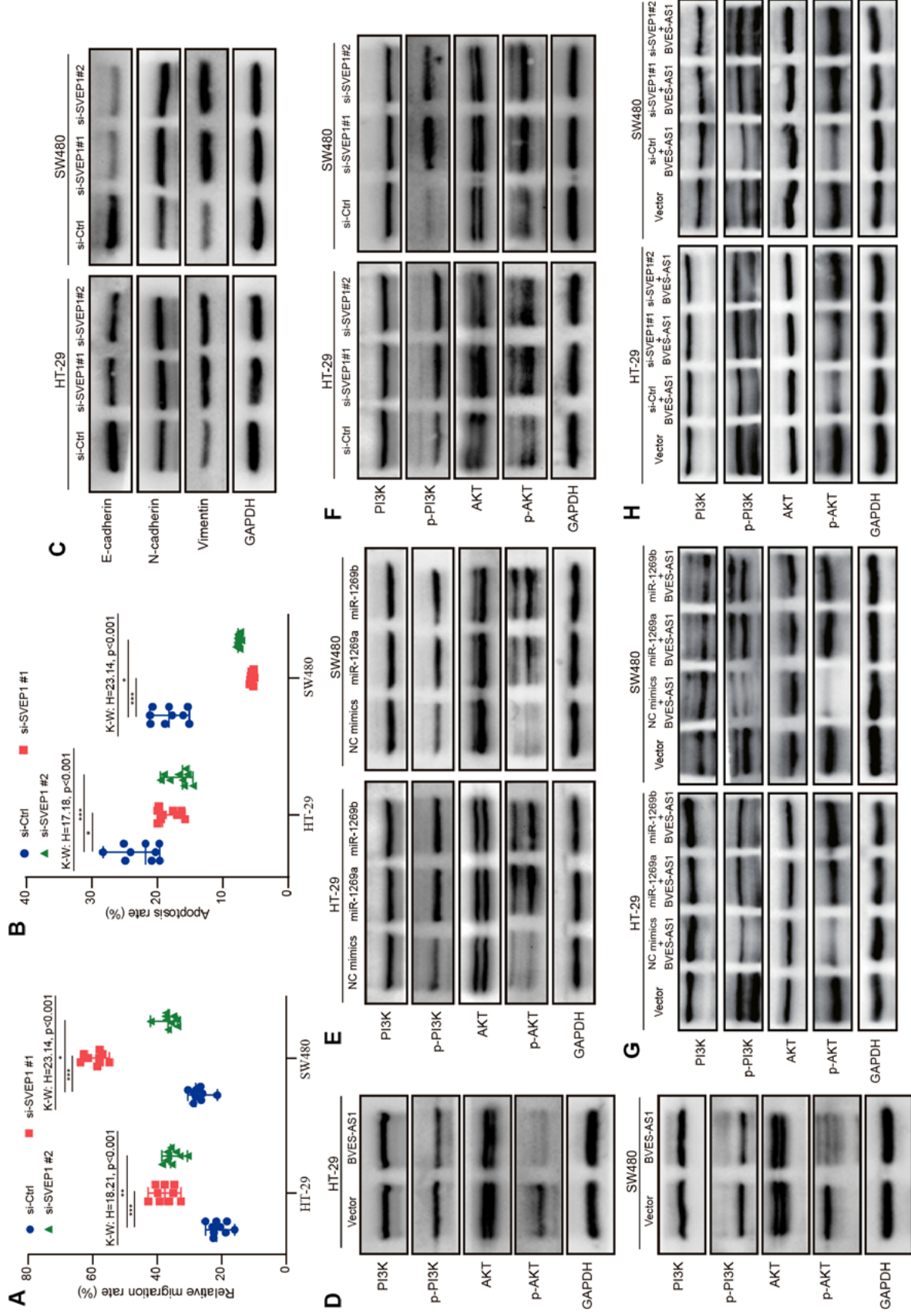


**Fig. 9. SVEP1 suppresses the proliferation, migration and invasion of colorectal cancer (CRC) cells in vitro.**  
**A.** Quantitative real-time polymerase chain reaction (qPCR) was used to detect the expression of *SVEP1* after transfecting siRNA; **B–E.** The proliferation of CRC cells transfected siRNA was accessed using Cell Counting Kit-8 (CCK-8) assay and 5-Ethynyl-2'-deoxyuridine (EdU) assay; **F–H.** The migration and invasion capability of HT-29 and SW480 cells after silencing *SVEP1* was evaluated with transwell and wound healing assays. A–C, E,G,H. \* $p < 0.05$ , \*\*\* $p < 0.01$ , \*\*\*\* $p < 0.001$ ; Kruskal–Wallis test with Dunn's post hoc test ( $n = 9$ ). The data are presented as median with range, and all assays were performed in triplicate

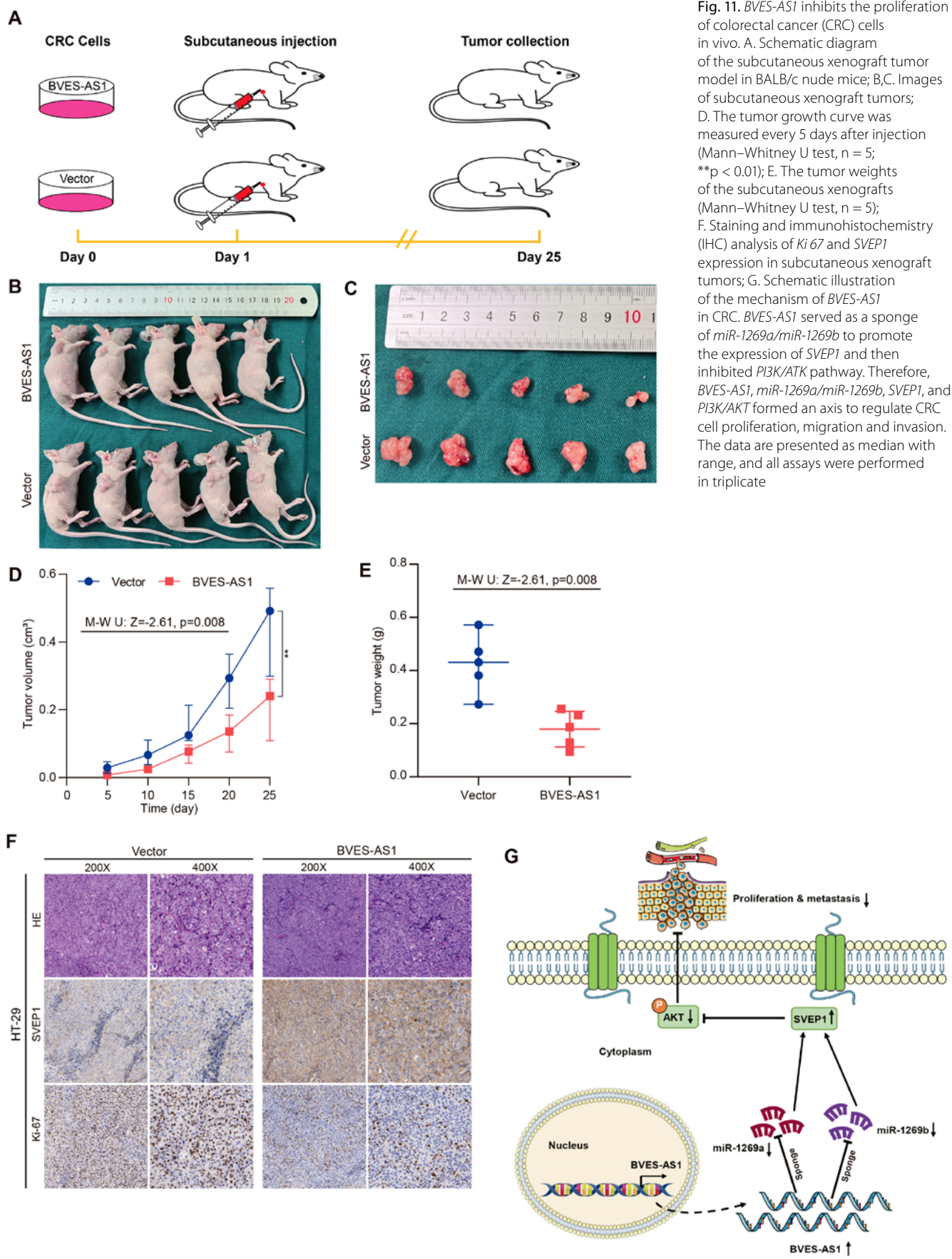


**Fig. 10.** *BVES-AS1* suppresses the *PI3K/AKT* pathway by *miR-1269a/miR-1269b* and *SVEP1*.

**A.** Wound healing assays was used to estimate colorectal cancer (CRC) cells migration abilities after knocking down *SVEP1*. **B.** Flow cytometry was used to detect the apoptosis of CRC cells after downregulating *SVEP1*; **C.** Western blot was used to estimate the relative protein levels of EMT markers (*E-cadherin*, *N-cadherin*, and *vimentin*) in CRC cells transfected with siRNA; **D–F.** The protein levels of *PI3K*, *p-PI3K*, *AKT*, and *p-AKT* in CRC cells with *BVES-AS1*, *miR-1269a/b* overexpression or *SVEP1* silence were detected with western blot; **G.H.** The protein levels of *PI3K*, *p-PI3K*, *AKT*, and *p-AKT* were detected with western blot after transfection of *miR-1269a/b* mimic or *SVEP1* siRNA in *BVES-AS1* overexpressed CRC cells. **A,B.** \* $p < 0.05$ , \*\*\* $p < 0.01$ , \*\*\*\* $p < 0.001$ ; Kruskal–Wallis test with Dunn's post hoc test ( $n = 9$ ). The data are presented as median with range, and all assays were performed in triplicate









The xenograft tumor weight of the *BVES-AS1* group was lower than that of the vector group (Fig. 11E). To evaluate the ability of *BVES-AS1* to induce tumor growth inhibition, H&E staining and IHC (*Ki-67*, *SVEP1*) were performed on subcutaneous xenograft tumors. The results showed that in xenograft tumors with *BVES-AS1* upregulation, *Ki-67* expression was decreased, and *SVEP1* expression was increased (Fig. 11F). Consistent with the in vitro experiments, the xenograft tumor assay indicated that *BVES-AS1* could suppress CRC cell growth in vivo.

## Discussion

To further understand the role of lncRNAs in the progression of CRC, we conducted bioinformatics analysis using TCGA data on paired tumor tissues and adjacent normal tissues from CRC patients. Our study revealed that *BVES-AS1* expression was significantly downregulated in human CRC. The low expression of *BVES-AS1* was associated with tumor infiltration depth and lymph node positivity in CRC patients. The overexpression of *BVES-AS1* suppresses the proliferation, invasion and EMT capability of CRC cells. *BVES-AS1* functioned as a sponge for *miR-1269a* and *miR-1269b*, regulating the expression of *SVEP1*. Additionally, *SVEP1* inhibits CRC cell proliferation and metastasis through the *PI3K/AKT* pathway. Ultimately, our study uncovered a complex regulatory network involving *BVES-AS1*, *miR-1269a/b*, *SVEP1*, and the *PI3K/AKT* pathway, collectively governing CRC progression.

*BVES-AS1* belongs to the antisense lncRNA family derived from the *BVES* antisense strand. lncRNAs can mediate biological functions through epigenetic, transcriptional and post-transcriptional regulation. The subcellular localization of lncRNAs determines their biological roles. lncRNAs localized in the cytoplasm regulate target genes mainly through competitive binding to miRNAs.<sup>6,23,24</sup> The results indicated that most of *BVES-AS1* was distributed in the SW480 and HT-29 cytoplasm, indicating that *BVES-AS1* can regulate the function of CRC through the ceRNA (competing for endogenous RNA) mechanism. Bioinformatics analysis showed that *miR-1269a* and *miR-1269b* shared the same seed region sequence and had potential binding sites to *BVES-AS1*. The *miR-1269a* expression was reportedly elevated in various cancers, and *miR-1269a* overexpression promoted tumor cell proliferation, metastasis and EMT.<sup>25–28</sup> Bu et al. revealed that *miR-1269a* enhanced the *TGF- $\beta$*  signaling pathway by competitively binding to *HOXD10* and *Smad7*, and *miR-1269a*-*HOXD10/Smad7*-*TGF- $\beta$*  built a positive feedback loop promoting CRC growth and metastasis.<sup>29</sup> *CircASS1* can sponge *miR-1269a* to regulate *VASH1* expression, inhibiting CRC cells growth and invasion ability.<sup>30</sup> Similarly, *miR-1269b* was upregulated in HCC, lung cancer and oropharyngeal squamous cell cancer.<sup>18,31,32</sup> However, overexpression of *miR-1269b* induced downregulation of *METTL3*, suppressing

stomach cancer cell proliferation and invasion.<sup>33</sup> Notably, there was no report on the expression and function of *miR-1269b* in CRC. Our experimental data indicated that *miR-1269a* and *miR-1269b* were elevated in CRC and had a negative relationship with *BVES-AS1* expression. Furthermore, as verified through molecular interaction experiments, *BVES-AS1* could serve as a miRNA sponge to interact with *miR-1269a* and *miR-1269b*.

As ceRNAs, lncRNAs perform biological functions mainly by targeting downstream mRNAs. We conducted RNA-seq, and the RNA-seq data indicated that *BVES-AS1* overexpression markedly upregulated *SVEP1* expression in CRC cells. The online database and dual-luciferase experiments predicted and validated that *SVEP1* was the common target of *miR-1269a* and *miR-1269b*. *SVEP1* is an extracellular matrix protein associated with epidermal differentiation and lymphatic vessel development and can act as a cell adhesion molecule involved in intercellular adhesion.<sup>34</sup> Its silencing enhanced cell chemotaxis and decreased epithelial marker expression and cell adhesion capacity.<sup>16,35</sup> Cell adhesion molecule degradation reduces the tumor adhesion ability, contributing to tumor cell separation from the primary region and metastasis.<sup>36</sup> *SVEP1* was expressed at relatively low levels in liver cancer and corresponded with invasion and metastasis. The proliferation, metastasis, bone invasion, and lung metastasis abilities were promoted by *SVEP1* downregulation in liver cancer cells.<sup>18,19</sup> We first revealed the biological function of *SVEP1* in CRC cells. The results suggested that *SVEP1* downregulation promoted CRC cell proliferation, migration, invasion, and EMT. The *PI3K/AKT* pathway is crucial in the proliferation, invasion, and apoptosis of various cancers.<sup>37</sup> *SVEP1* knockdown induced the upregulation of phosphorylated *AKT*, thus promoting HCC cell proliferation and metastasis.<sup>18</sup> Our research also demonstrated that *SVEP1* downregulation could activate p-*PI3K* and p-*AKT* expression. In addition, overexpression of *BVES-AS1* partially reversed the upregulation of phosphorylated *PI3K* and *AKT* induced by *SVEP1* silencing. These data suggested that *BVES-AS1* overexpression suppressed CRC cell proliferation and invasion by sponging *miR-1269a/miR-1269b* to upregulate *SVEP1* expression and inhibit the activation of the *PI3K/AKT* pathway.

## Limitations

Although the tumor suppressive effect and mechanism of *BVES-AS1* were revealed in CRC, some limitations must be considered. First, the study showed that *BVES-AS1* was expressed in the nucleus and cytoplasm of CRC cells. We only investigated the molecular mechanism of *BVES-AS1* in the cytoplasm; the function of nuclear *BVES-AS1* needs to be further verified. Second, *BVES-AS1* was able to serve as a ceRNA to sponge *miR-1269a* and *miR-1269b*. However, in CRC cells, the relationship between *miR-1269a* and *miR-1269b* remains unclear. Finally, we suggest that *SVEP1* knockdown contributes to the activation

of the *PI3K/AKT* pathway. Nevertheless, the specific mechanism by which *SVEP1* regulates the *PI3K/AKT* pathway needs to be further elucidated.

## Conclusions

This study suggests that *BVES-AS1* functions as a tumor suppressor gene inhibiting the growth and metastasis of CRC cells in vivo and in vitro. Mechanistically, *BVES-AS1* acts as a miRNA sponge, attenuating the effects of *miR-1269a* and *miR-1269b* on *SVEP1*, which in turn inhibits the *PI3K/AKT* pathway. Therefore, our study reveals that the *BVES-AS1-miR-1269a/b-SVEP1-PI3K/AKT* axis is a key regulator in suppressing CRC progression. These findings provide new insights for potential treatment strategies in CRC.

## Supplementary data

The supplementary materials are available at <https://doi.org/10.5281/zenodo.10069707>. The package contains the following files:

Supplementary Table 1. Sequences of oligonucleotides and probes used in this study.

Supplementary Table 2. Primer sequences.

Supplementary Table 3. Clinical characteristics of colorectal cancer patients.

Supplementary Table 4. Differentially expressed genes in RNA-seq.

Supplementary Table 5. Results of normality test.

Supplementary Table 6. Statistical analysis results of models.

Supplementary Table 7. Results of Levene's test.

Supplementary Fig. 1. *BVES-AS1* inhibits CRC cell proliferation, migration and invasion in vitro.

Supplementary Fig. 2. *BVES-AS1* reverses the oncogenic effect of *miR-1269a* or *miR-1269b*.

Supplementary Fig. 3. *SVEP1* inhibits CRC cell proliferation, migration, and invasion in vitro.

## Data availability


The datasets generated and/or analyzed during the current study are available from the corresponding author on reasonable request.

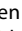
## Consent for publication


Not applicable.


## ORCID iDs

Jianguo Yang  <https://orcid.org/0000-0000-0000-0000>

Qican Deng  <https://orcid.org/0000-0003-4233-970X>

Zhenzhou Chen  <https://orcid.org/0000-0002-4324-5388>

Yajun Chen  <https://orcid.org/0000-0002-4059-6561>

Zhongxue Fu  <https://orcid.org/0000-0001-8160-2975>

## References

- Sung H, Ferlay J, Siegel RL, et al. Global cancer statistics 2020: GLOBOCAN estimates of incidence and mortality worldwide for 36 cancers in 185 countries. *CA A Cancer J Clin*. 2021;71(3):209–249. doi:10.3322/caac.21660
- Lu B, Li N, Luo CY, et al. Colorectal cancer incidence and mortality: The current status, temporal trends and their attributable risk factors in 60 countries in 2000–2019. *Chin Med J (Engl)*. 2021;134(16):1941–1951. doi:10.1097/CM9.0000000000001619
- Xie YH, Chen YX, Fang JY. Comprehensive review of targeted therapy for colorectal cancer. *Sig Transduct Target Ther*. 2020;5(1):22. doi:10.1038/s41392-020-0116-z
- Maeda H, Kashiwabara K, Aoyama T, et al. Hazard rate of tumor recurrence over time in patients with colon cancer: Implications for post-operative surveillance from three Japanese Foundation for Multidisciplinary Treatment of Cancer (JFMC) clinical trials. *J Cancer*. 2017;8(19):4057–4064. doi:10.7150/jca.21365
- Statello L, Guo CJ, Chen LL, Huarte M. Gene regulation by long non-coding RNAs and its biological functions. *Nat Rev Mol Cell Biol*. 2021;22(2):96–118. doi:10.1038/s41580-020-00315-9
- Kopp F, Mendell JT. Functional classification and experimental dissection of long noncoding RNAs. *Cell*. 2018;172(3):393–407. doi:10.1016/j.cell.2018.01.011
- Wang X, Cheng H, Zhao J, et al. Long noncoding RNA DLGAP1-AS2 promotes tumorigenesis and metastasis by regulating the Trim21/ELOA/LHPP axis in colorectal cancer. *Mol Cancer*. 2022;21(1):210. doi:10.1186/s12943-022-01675-w
- Shi K, Yang S, Chen C, et al. RNA methylation-mediated LINC01559 suppresses colorectal cancer progression by regulating the miR-106b-5p/PTEN axis. *Int J Biol Sci*. 2022;18(7):3048–3065. doi:10.7150/ijbs.70630
- Wang L, Cho KB, Li Y, Tao G, Xie Z, Guo B. Long noncoding RNA (lncRNA)-mediated competing endogenous RNA networks provide novel potential biomarkers and therapeutic targets for colorectal cancer. *Int J Mol Sci*. 2019;20(22):5758. doi:10.3390/ijms20225758
- Xu W, Zhou G, Wang H, et al. Circulating lncRNA SNHG11 as a novel biomarker for early diagnosis and prognosis of colorectal cancer. *Int J Cancer*. 2020;146(10):2901–2912. doi:10.1002/ijc.32747
- Nikolaou S, Qiu S, Fiorentino F, Rasheed S, Tekkis P, Kontovounisios C. Systematic review of blood diagnostic markers in colorectal cancer. *Tech Coloproctol*. 2018;22(7):481–498. doi:10.1007/s10151-018-1820-3
- Gilgès D, Vinit MA, Callebaut I, et al. Polydom: A secreted protein with pentraxin, complement control protein, epidermal growth factor and von Willebrand factor A domains. *Biochem J*. 2000;352(Pt 1):49–59. PMID:11062057. PMCID:PMC1221431.
- Sato-Nishiuchi R, Nakano I, Ozawa A, et al. Polydom/SVEP1 is a ligand for integrin  $\alpha\beta 1$ . *J Biol Chem*. 2012;287(30):25615–25630. doi:10.1074/jbc.M112.355016
- Karpanen T, Padberg Y, Van De Pavert SA, et al. An evolutionarily conserved role for Polydom/Svep1 during lymphatic vessel formation. *Circ Res*. 2017;120(8):1263–1275. doi:10.1161/CIRCRESAHA.116.308813
- Morooka N, Futaki S, Sato-Nishiuchi R, et al. Polydom is an extracellular matrix protein involved in lymphatic vessel remodeling. *Circ Res*. 2017;120(8):1276–1288. doi:10.1161/CIRCRESAHA.116.308825
- Samuelov L, Li Q, Bochner R, et al. SVEP 1 plays a crucial role in epidermal differentiation. *Exp Dermatol*. 2017;26(5):423–430. doi:10.1111/exd.13256
- Glaite-Santar C, Pasmanik-Chor M, Benayahu D. Expression pattern of SVEP1 alternatively-spliced forms. *Gene*. 2012;505(1):137–145. doi:10.1016/j.gene.2012.05.015
- Chen L, Liu D, Yi X, et al. The novel miR-1269b-regulated protein SVEP1 induces hepatocellular carcinoma proliferation and metastasis likely through the PI3K/Akt pathway. *Cell Death Dis*. 2020;11(5):320. doi:10.1038/s41419-020-2535-8
- Gong WC, Han ZQ, Guo MX, et al. Decreased expression of SVEP1 is closely related to a cancer stem cell-like phenotype and poor prognosis in hepatocellular carcinoma. *Neoplasia*. 2022;69(5):1209–1216. doi:10.4149/neo\_2022\_220614N629
- Wu J, Cai Y, Zhao G, Li M. A ten N6-methyladenosine-related long non-coding RNAs signature predicts prognosis of triple-negative breast cancer. *Clin Lab Anal*. 2021;35(6):e23779. doi:10.1002/jcla.23779

21. Xing Y, Zhao Z, Zhu Y, Zhao L, Zhu A, Piao D. Comprehensive analysis of differential expression profiles of mRNAs and lncRNAs and identification of a 14-lncRNA prognostic signature for patients with colon adenocarcinoma. *Oncol Rep.* 2018;39(5):2365–2375. doi:10.3892/or.2018.6324
22. Lu S, Han L, Hu X, et al. N6-methyladenosine reader IMP2 stabilizes the ZFAS1/OLA1 axis and activates the Warburg effect: Implication in colorectal cancer. *J Hematol Oncol.* 2021;14(1):188. doi:10.1186/s13045-021-01204-0
23. Yao RW, Wang Y, Chen LL. Cellular functions of long noncoding RNAs. *Nat Cell Biol.* 2019;21(5):542–551. doi:10.1038/s41556-019-0311-8
24. Salmena L, Poliseno L, Tay Y, Kats L, Pandolfi PP. A ceRNA hypothesis: The Rosetta Stone of a hidden RNA language? *Cell.* 2011;146(3):353–358. doi:10.1016/j.cell.2011.07.014
25. Cho HJ, Baek GO, Seo CW, et al. Exosomal microRNA-4661-5p-based serum panel as a potential diagnostic biomarker for early-stage hepatocellular carcinoma. *Cancer Med.* 2020;9(15):5459–5472. doi:10.1002/cam4.3230
26. Guo X, Dai X, Liu J, Cheng A, Qin C, Wang Z. Circular RNA circREPS2 acts as a sponge of miR-558 to suppress gastric cancer progression by regulating RUNX3/ $\beta$ -catenin signaling. *Mol Ther Nucleic Acids.* 2020;21:577–591. doi:10.1016/j.omtn.2020.06.026
27. Zhang K, Zhang L, Mi Y, et al. A ceRNA network and a potential regulatory axis in gastric cancer with different degrees of immune cell infiltration. *Cancer Sci.* 2020;111(11):4041–4050. doi:10.1111/cas.14634
28. Zhao Y, Xu L, Wang X, Niu S, Chen H, Li C. A novel prognostic mRNA/miRNA signature for esophageal cancer and its immune landscape in cancer progression. *Mol Oncol.* 2021;15(4):1088–1109. doi:10.1002/1878-0261.12902
29. Bu P, Wang L, Chen KY, et al. miR-1269 promotes metastasis and forms a positive feedback loop with TGF- $\beta$ . *Nat Commun.* 2015;6(1):6879. doi:10.1038/ncomms7879
30. Xiong HL, Zhong XH, Guo XH, Liao HJ, Yuan X. circASS1 overexpression inhibits the proliferation, invasion and migration of colorectal cancer cells by regulating the miR-1269a/VASH1 axis. *Exp Ther Med.* 2021;22(4):1155. doi:10.3892/etm.2021.10589
31. Yang W, Xiao W, Cai Z, Jin S, Li T. miR-1269b drives cisplatin resistance of human non-small cell lung cancer via modulating the PTEN/PI3K/AKT signaling pathway. *Onco Targets Ther.* 2020;13:109–118. doi:10.2147/OTT.S225010
32. Chen HC, Tseng YK, Chi CC, et al. Genetic variants in microRNA-146a (C > G) and microRNA-1269b (G > C) are associated with the decreased risk of oral premalignant lesions, oral cancer, and pharyngeal cancer. *Arch Oral Biol.* 2016;72:21–32. doi:10.1016/j.archoralbio.2016.08.010
33. Kang J, Huang X, Dong W, Zhu X, Li M, Cui N. MicroRNA-1269b inhibits gastric cancer development through regulating methyltransferase-like 3 (METTL3). *Bioengineered.* 2021;12(1):1150–1160. doi:10.1080/21655979.2021.1909951
34. Morris GE, Denniff MJ, Karamanavi E, et al. The integrin ligand SVEP1 regulates GPCR-mediated vasoconstriction via integrins  $\alpha 9\beta 1$  and  $\alpha 4\beta 1$ . *Br J Pharmacol.* 2022;179(21):4958–4973. doi:10.1111/bph.15921
35. Nakada TA, Russell JA, Boyd JH, Thair SA, Walley KR. Identification of a nonsynonymous polymorphism in the *SVEP1* gene associated with altered clinical outcomes in septic shock. *Crit Care Med.* 2015;43(1):101–108. doi:10.1097/CCM.0000000000000604
36. Özkan E, Chia PH, Wang RR, et al. Extracellular architecture of the SYG-1/SYG-2 adhesion complex instructs synaptogenesis. *Cell.* 2014;156(3):482–494. doi:10.1016/j.cell.2014.01.004
37. Koveitypour Z, Panahi F, Vakilian M, et al. Signaling pathways involved in colorectal cancer progression. *Cell Biosci.* 2019;9(1):97. doi:10.1186/s13578-019-0361-4